# The investigation of donor-acceptor compatibility in bulk-heterojunction polymer systems

Jen-Hsien Huang,[1] Yu-Sheng Hsiao,[1] Eric Richard,[2] Chun-Chao Chen,[2] Peilin Chen,[1] Gang Li,[2,a)] Chih-Wei Chu,[1,3,a)] and Yang Yang[2,a)]
[1]*Research Center for Applied Sciences, Academia Sinica, Taipei 11529, Taiwan*
[2]*Department of Materials Science and Engineering, University of California-Los Angeles, Los Angeles, California 90095, USA*
[3]*Department of Photonics, National Chiao Tung University, Hsinchu 300, Taiwan*

(Received 21 February 2013; accepted 1 July 2013; published online 23 July 2013)

The fullerene derivative, indene-$C_{60}$ bisadduct (ICBA), has been introduced into poly(3-hexylthiophene) (P3HT) to improve the efficiency of P3HT-based devices. However, we found that ICBA is not suitable for most low bandgap polymers. In this study, we have correlated the cell performance with surface energy between the donor and acceptor materials in a bulk-heterojunction cell. These results show that higher photocurrent can be attributed to the morphology improvement induced by larger surface energy difference ($\Delta\gamma$) between the low bandgap polymer and fullerene. These results also suggest that synthetic strategies which adjust the $\Delta\gamma$ between donor and acceptor should be considered. © *2013 AIP Publishing LLC*. [http://dx.doi.org/10.1063/1.4816056]

Due to their advantages of flexibility, availability of raw materials, and ease of processing, polymeric bulk-heterojunction (BHJ) solar cells are a promising technology for providing cost-effective energy in the future.[1–4] Among many high performance polymers, poly(3-hexylthiophene) (P3HT) is one of the most studied donor materials (bandgap 1.9 eV) for polymer solar cells (PSCs). In addition, many lower bandgap polymer materials have been reported for harvesting more solar energy.[5–13] In donor/acceptor based organic solar cells, the *V*oc is correlated to the offset between energy levels of the highest occupied molecular orbital (HOMO) of the donor and lowest unoccupied molecular orbital (LUMO) of the acceptor.[14] The photocurrent is associated with the absorption of the polymer and acceptor, and the associated charge carrier mobility and morphology characteristics such as the degree of mixing between the polymer and fullerene, phase separation, and the formation of percolation pathways. A recent advancement of the PSC is the acceptor indene-$C_{60}$ bisadduct (ICBA), which has a higher LUMO energy level than [6,6]-phenyl-$C_{61}$-butyric acid methyl ester (PCBM).[15–17] As a result, the $V_{OC}$ of P3HT-based devices can be increased from 0.60 to 0.84 V and power conversion efficiency (PCE) is around 6.5%.[13]

However, on low bandgap polymers, such as poly[4,8-bis-substituted-benzo[1,2-b:4,5-b0] dithiophene-2,6-diyl-alt-4-substituted-thieno[3, 4-b]thiophene-2,6-diyl] derivative (PBDTTT-C),[8,18] the effect of ICBA is strongly system dependent. In the PBDTTT-C:ICBA system, the $V_{OC}$ indeed increased as expected, but the $J_{SC}$ dropped significantly, leading to a lower PCE (The *J*–*V* curves are shown in supplementary material,[39] Fig. S1). This is somehow surprising as the LUMO difference of donor and acceptor is 0.4 eV,[15,18] which is expected to be enough to provide driving force for exciton dissociation.[14] On the other hand, the silicon-bridged cyclopenta-dithiophene (CPDT)-based polymer, poly[(4,4′-bis(2-ethylhexyl)dithieno[3,2-b:2′,3′-d]silole)-2,6-diyl-*alt*-(5,5′-thienyl-4,4′-dihexyl-2,2′-bithiazole)-2,6-diyl] (PSPDTTBT),[19] shows both $V_{OC}$ and $J_{SC}$ increase significantly. These results clearly indicate that the HOMO and LUMO levels of the electron donor and acceptor alone cannot be fully responsible for the prediction of device performance.

We speculate that the difference in performance between these polymer blends comes from the compatibility of the polymer/ICBA system in morphology formation. In this work, we investigate the compatibility of the PCBM/ICBA:donor (PSPDTTBT and P3HT) blends and the effect on PSC device. A comprehensive investigation of the active layer film properties of PSPDTTBT blended with PCBM and ICBA acceptors has been conducted. Atomic force microscopy (AFM), transmission electron microscopy (TEM), and exciton lifetime (ELT) mapping of the film morphology were used in this work to characterize the active layer morphology. The information obtained allowed us to understand the difference of ICBA on the morphologies based on P3HT and PSPDTTBT films.

The PSPDTTBT was synthesized using the method reported previously.[19] P3HT, PCBM, and ICBA were purchased by Rieke Metals, Nano−C, and Lumitech, respectively. The active layer of polymer:fullerene (1:1 w/w, 2% in 1,2,-dichlorobenzene) was spin-coated on poly(ethylenedioxythiophene):polystyrene sulfonate (PEDOT:PSS) modified ITO substrate. A bilayer electrode–calcium (20 nm) and aluminum (100 nm) was evaporated on top of the polymer films. The device active area was 0.1 $cm^2$. Single carrier devices (electron-and hole-only) were fabricated to study the carrier transport properties. In the hole-only devices, Ca was replaced with $MoO_3$ with high work function ($\Phi = 5.3$ eV). For the electron-only devices, the PEDOT:PSS layer was replaced with $Cs_2CO_3$ ($\Phi = 2.9$ eV).

The cells were tested under simulated AM 1.5G irradiation at 100 mW $cm^{-2}$ using a Xe arc lamp-based solar simulator (Thermal Oriel 1000 W). The light intensity was calibrated using a mono-silicon photodiode equipped with a

a)Authors to whom correspondence should be addressed. Electronic addresses: gangl@ucla.edu, gchu@gate.sinica.edu.tw, and yangy@ucla.edu

 

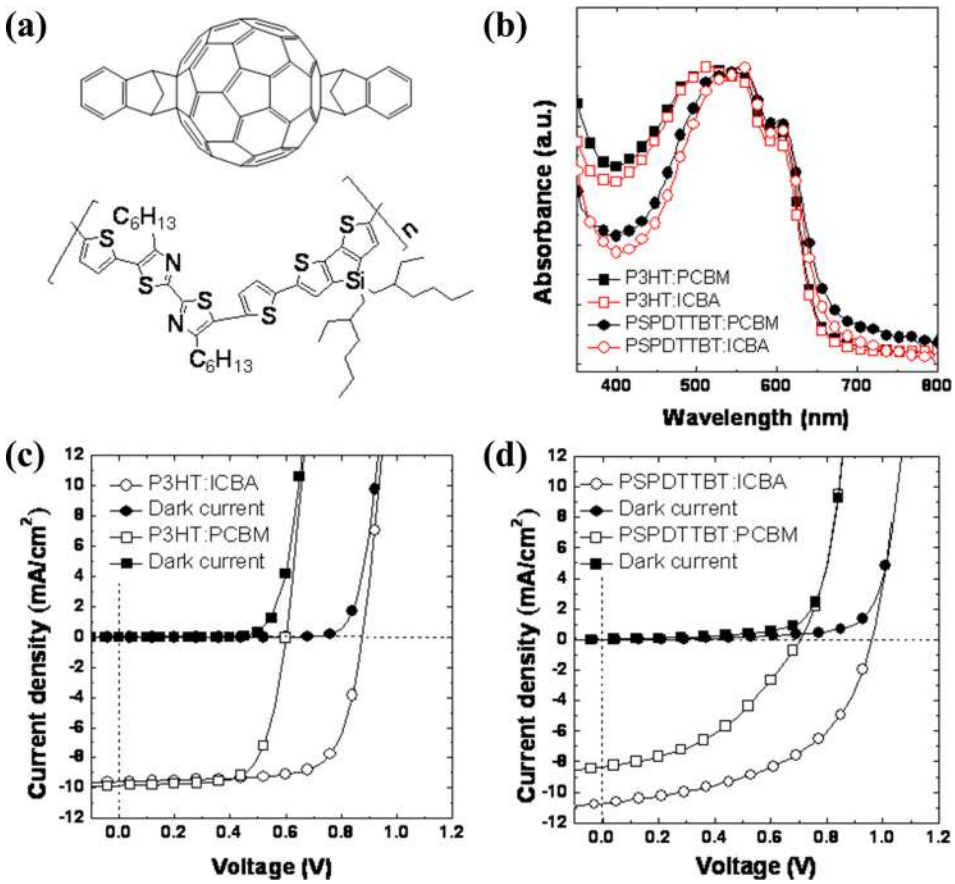


FIG. 1. (a) The chemical structure of ICBA and PSPDTTBT. (b) UV–vis absorption of P3HT:PCBM, P3HT:ICBA, PSPDTTBT:PCBM, and PSPDTTBT:ICBA films. (c) Photo and dark current of the P3HT:PCBM and P3HT:ICBA BHJ solar cells. (d) Photo and dark current of the PSPDTTBT:PCBM and PSPDTTBT:ICBA BHJ solar cells.

KG-5 color filter. The surface morphologies of the polymer films were investigated using AFM (Digital Instrument NS 3a controller equipped with a D3100 stage). TEM images were taken by a JOEL JEM-1230 microscope operating at 80 keV accelerating voltage. In the fluorescence lifetime measurement, the samples were excited with 470 nm wavelength light from a picosecond laser (LDH-P-C-470, PicoQuant); the fluorescence lifetime signal was measured using time-correlated single photon counting (TCSPC).

The chemical structures of PSPDTTBT and ICBA are presented in Fig. 1(a).[19] Fig. 1(b) shows the film absorbance of the P3HT and PSPDTTBT blended with PCBM and ICBA. Both P3HT and PSPDTTBT blended with ICBA have similar absorbance spectra to their blends with PCBM. However, the photocurrent is very different as shown in Figs. 1(c) and 1(d). For P3HT-based devices, the $J_{SC}$ values are almost the same (9.58 vs. 9.85 mA/cm$^2$). With fill factors (FFs) of 69.4% and 73.0% and $V_{OC}$ values of 0.60 and 0.87 V, the PCEs for P3HT:PCBM and P3HT:ICBA are 4.10% and 6.09%, respectively. On the other hand, the $J_{SC}$ for PSPDTTBT devices increases significantly from 8.34 to 10.69 mA/cm$^2$ when switched from PCBM to ICBA. The FF also exhibits a significant enhancement (42.3% to 51.3%). This leads to 5.21% PCE of PSPDTTBT:ICBA is vs. 2.50% in PSPDTTBT:PCBM devices.

The TEM and AFM images for the PSPDTTBT:PCBM and PSPDTTBT:ICBA films are shown in Fig. 2. Typical bright-field TEM images for PSPDTTBT:PCBM and PSPDTTBT:ICBA films are shown in Figs. 2(a) and 2(b), respectively. The image of the PSPDTTBT:PCBM film reveals a well-mixed morphology without obvious phase separation. In contrast, the most pronounced feature of PSPDTTBT:ICBA compared to its PCBM counterpart is the appearance of continuous dark pathways across the film with high contrast to the background. Following Yang's morphology work of P3HT:fullerene solar cell,[20] the dark regions in

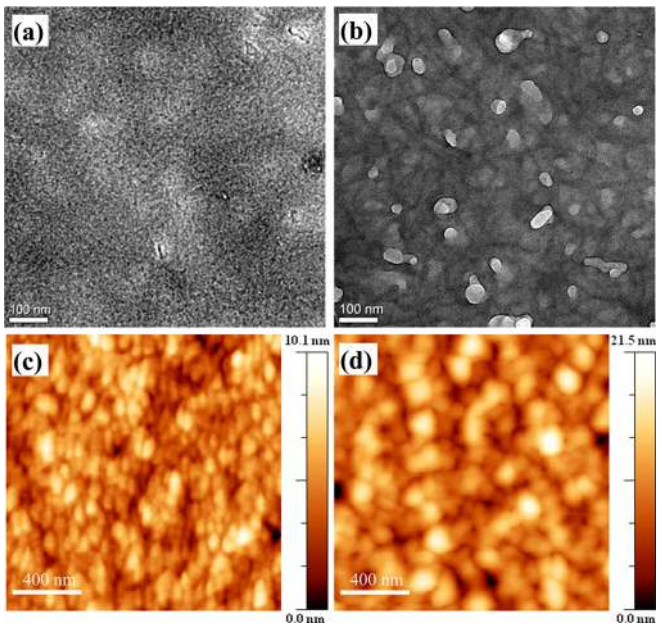


FIG. 2. (a) TEM images of (a) PSPDTTBT:PCBM and (b) PSPDTTBT:ICBA BHJ films. The blend films were spin cast on PEDOT:PSS modified glass substrate and then the film was floated on a water surface. (b) AFM surface morphology of (c) PSPDTTBT:PCBM and (d) PSPDTTBT:ICBA BHJ films. Scale bars: 400 nm.

Fig. 2(b) are identified as ICBA clusters. Moreover, the bright regions are larger and have higher contrast in the ICBA blend, suggesting that the crystallinity of PSPDTTBT has also been improved. Corresponding changes in the surface topography were also seen by AFM, as shown in Figs. 2(c) and 2(d). The film with PCBM is much smoother, with RMS roughness of 1.21 nm, while the ICBA containing film has RMS roughness of 2.34 nm. The domain sizes estimated by AFM topology images are ~20–70 and 50–110 nm for PSPDTTBT:PCBM and PSPDTTBT:ICBA films, respectively. This is consistent with the higher crystallinity of PSPDTTBT:ICBA inferred from TEM images. The higher photocurrent and FF obtained in PSPDTTBT:ICBA devices seems to be the result of the formation of an interpenetrating network and better charge transport. In contrast, P3HT gives similar internal and surface morphologies when blended with PCBM or ICBA (The TEM and AFM images are shown in supplementary material,[39] Fig. S2) and the $J_{SC}$ and FF for P3HT:PCBM and P3HT:ICBA devices are also similar.

In order to study the lateral variation in ELT in the films, we used confocal microscopy combined with a florescence lifetime module to make 2D ELT maps.[21,22] This information allows us to correlate the morphology with the ELT distribution on the nanoscale. Figs. 3(a) and 3(b) show the ELT images of films PSPDTTBT:PCBM and PSPDTTBT:ICBA films. These data provide information hidden from the surface examination in Fig. 2. In the ELT mapping images, the red, blue, and green-yellow regions correspond to long, short, and intermediate ELT which we attribute to donor-rich (polymer), acceptor-rich (PCBM or ICBA), and well-mixed domains[23] (Fig. 3(e)). The calculated ELT for the marked red and blue regions in Fig. 3(b) is 2.63 and 2.30 ns, respectively. The well mixed region reveals much lower photoluminescence intensity due to the ultrafast photoinduced charge transfer from the polymer to fullerene[23] and thus effective exciton dissociation. In Fig. 3(a), the ELT images of the PSPDTTBT:PCBM film reveal a much more homogeneous ELT distribution compared with that of PSPDTTBT:ICBA. The PSPDTTBT:ICBA film displays more pronounced red and blue regions, indicating the formation of PSPDTTBT and ICBA phase separation. To quantify the variations in photoluminescence quenching, we fitted the resulting ELD images with a Gaussian function (Figs. 3(c) and 3(d)) and obtained an average lifetime for PSPDTTBT:PCBM and PSPDTTBT:ICBA as 2.41 and 2.36 ns, with an ELD distribution ranging from 2.23–2.64 ns to 2.02–2.79 ns, respectively. For comparison, the average lifetime of pure PSPDTTBT is 3.54 ns (the ELD image of pristine PSPDTTBT is shown in supplementary material,[39] Fig. S3). The broadened ELT distribution of PSPDTTBT:ICBA indicates the presence of enhanced compositional separation

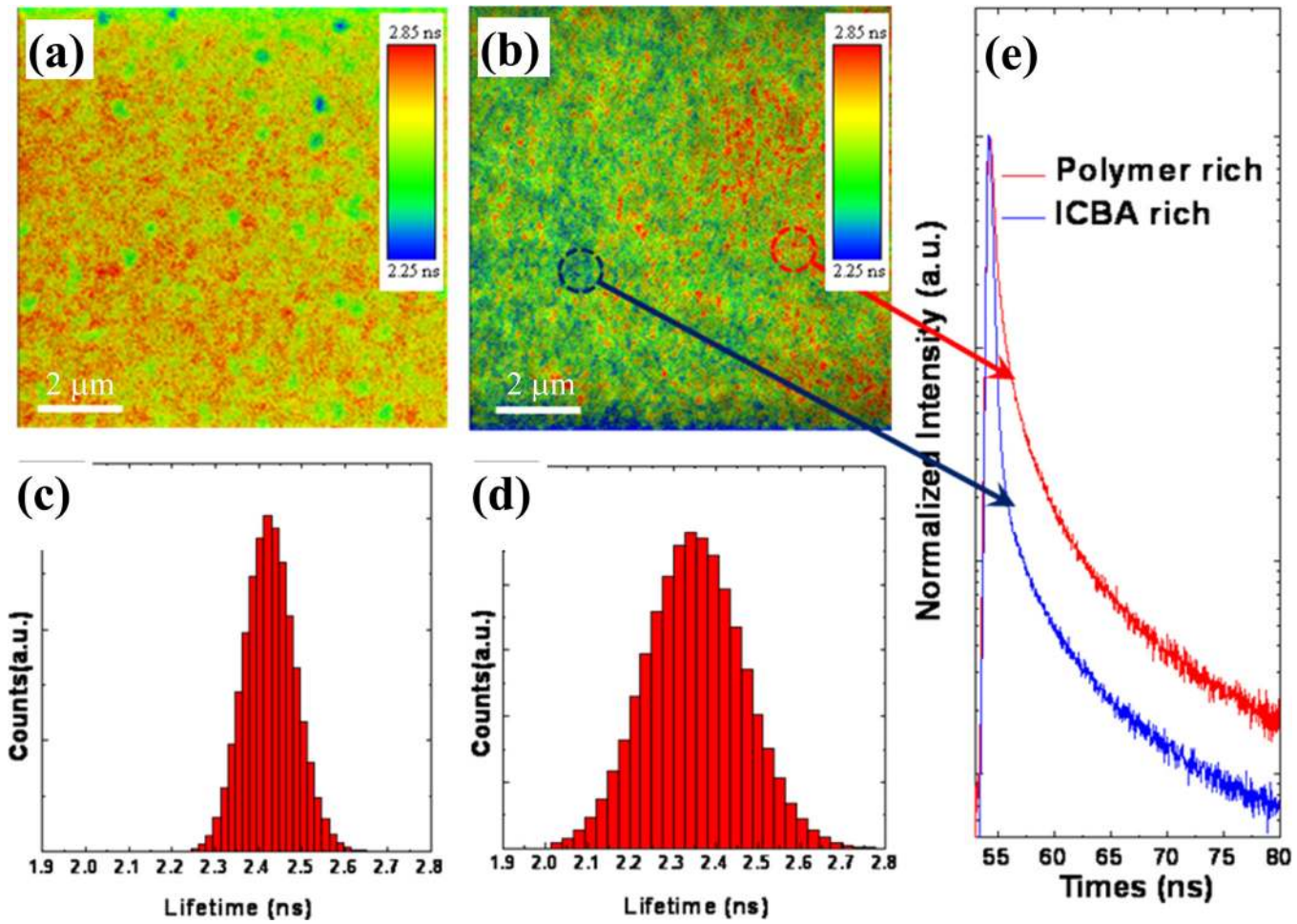


FIG. 3. (a) and (b) ELT mapping of PSPDTTBT:PCBM and PSPDTTBT:ICBA BHJ films and (c) and (d) histograms of the ELT for PSPDTTBT:PCBM and PSPDTTBT:ICBA BHJ films, respectively. (e) Photoluminescence lifetime decay curves of the marked region in Fig. 3(b). The ELT mapping was measured after excitation at 470 nm using a picosecond laser microscope (512 × 512 pixels). Scale bars: 2 $\mu$m.

within the blended films. The phase separation and favorable morphology revealed by the ELT and TEM images thus agree with the improved $J_{SC}$ and FF. In the cases of P3HT:PCBM and P3HT:ICBA, the ELT images (Fig. S4)[19] are very similar. In both cases, well separated polymer and acceptor domains were formed with domain size ~150–200 nm, which is consistent with the morphology from TEM and similar $J_{SC}$ and FF in device (the ELT images are shown in supplementary material,[39] Fig. S4).

The space-charge limited current (SCLC) model was used to determine the carrier mobility. Figs. 4(a) and 4(b) show the current-voltage ($J$–$V$) characteristics of electron- and hole-only devices. Based on the fitting of the dark current by the SCLC model, $J = 9\varepsilon_0\varepsilon_r\mu V^2/8L^3$,[24] the electron and hole mobility for PSPDTTBT:PCBM are determined to be $5.42 \times 10^{-8}$ and $1.9 \times 10^{-9}$ m$^2$/Vs. For PSPDTTBT:ICBA, they are $8.62 \times 10^{-9}$ and $9.5 \times 10^{-9}$ m$^2$/Vs, respectively. The larger electron mobility of the PSPDTTBT:PCBM device results from the larger intrinsic mobility of PCBM compared to that of ICBA. The corresponding field-effect mobilities of PCBM and ICBA were found to be $4.01 \times 10^{-6}$ and $2.80 \times 10^{-9}$ m$^2$/Vs (the characteristics of field-effect transistor are shown in supplementary material,[39] Fig. S5). Interestingly, the field-effect mobility of PCBM is larger than that of ICBA by three orders of magnitude. However, the results fitted from SCLC model reveal the electron mobility of PSPDTTBT:PCBM is only larger than the ICBA counterpart by one order of magnitude. This is believed due to the favorable morphology developed within the PSPDTTBT:ICBA film with percolating pathways of ICBA, which leads to a larger electron mobility which compensates the electron mobility difference between PCBM and ICBA based devices. For the same reason, the ICBA based device also shows a higher hole mobility which leads to a highly balanced carrier transport ($\mu_e/\mu_h = 0.91$), comparing to a ratio of 28 in PSPDTTBT:PCBM case. The balanced carrier transport[25] agrees with the enhanced fill factor in the PSPDTTBT:ICBA device.

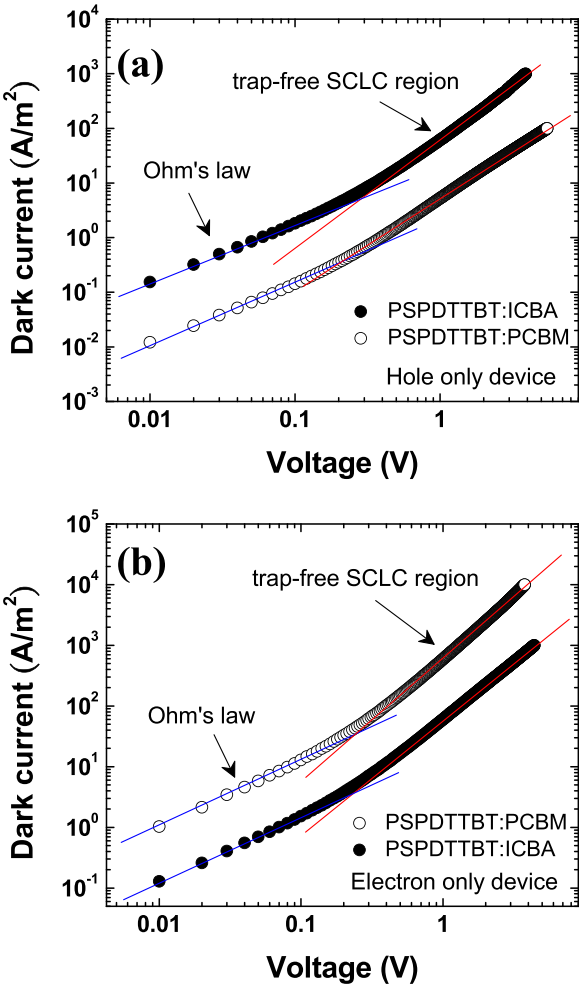


FIG. 4. Measured $J$–$V$ characteristics under dark for (a) electron-only and (b) hole only PSPDTTBT:PCBM and PSPDTTBT:ICBA BHJ devices. The slopes of Ohm'law and SCLC region are one and two, respectively.

To understand the origin of the very different morphology and OPV device performance in polymer-fullerene combination, we investigated the compatibility of polymer-fullerene through surface energy analysis. Surface energy has been shown to be critical to the morphology formation in polymer solar cell active layer. For example, it has been demonstrated that vertical phase separation occurs within the P3HT:PCBM films.[26–31] The surface segregation is driven by the total energy minimization of the system, which is mainly due to the difference in surface energy ($\gamma$) of P3HT and PCBM with respect to that of the substrate and environment. Germack *et al*. show that the buried interface composition of P3HT:PCBM blend can be tuned either to be P3HT rich using low $\gamma$ OTS8 coated substrate or to PCBM rich using high $SiO_2$ substrate.[31]

We expect the same principle may also apply in nanoscale BHJ morphology formation. The contact angles of polymers and fullerene derivatives were measured to evaluate the $\gamma$ (Table I). The contact angles were measured with water, ethylene glycol, and diiodomethane. The $\gamma$ was calculated through the geometric mean approximation. The surface energy of polymers (PSPDTTBT, PBDTTT-C, P3HT) and fullerenes (PCBM and ICBA) are estimated to be 44.22, 23.97, 26.42, 31.74, and 21.71 mJ/m$^2$, respectively. For P3HT, its surface energy is in between of PCBM and ICBA. The $|\Delta\gamma|$ between P3HT and PCBM is close to that between P3HT and ICBA (5.32 vs. 4.71 mJ/m$^2$). Therefore, similar $|\Delta\gamma|$ results in almost the same morphology for P3HT:PCBM and P3HT:ICBA blends. For PSPDTTBT, its surface energy is larger than that of both PCBM and ICBA. The values of

TABLE I. Summary of the contact angle for water, ethylene glycol, and diiodomethane and their corresponding surface energy ($\gamma$) of PSPDTTBT, P3HT, PBDTTT-C, PCBM, and ICBA. The $\gamma$ was calculated through the geometric mean approximation.

| | Contact angle (deg) | | | |
|---|---|---|---|---|
| | Water | Ethylene glycol | Diiodomethane | $\gamma$[a] (mJ/m$^2$) |
| PSPDTTBT | 83.5 | 63.5 | 19.6 | 44.22 |
| PBDTTT-C (Ref. 9) | 113.0 | 89.3 | 69.4 | 23.97 |
| P3HT | 111.3 | 87.4 | 63.8 | 26.42 |
| PCBM[b] | 101.2 | 65.5 | … | 31.74 |
| ICBA[b] | 105.0 | 78.3 | … | 21.71 |

[a]The surface energy are obtained from the contact angle measurement.
[b]The contact angle for diiodomethane of PCBM and ICBA cannot be measured due to their high dissolubility in diiodomethane.

$\Delta\gamma$ for PSPDTTBT and PCBM and PSPDTTBT and ICBA are quite different (12.48 vs. 22.51 mJ/m$^2$), leading to significantly different morphologies. The much smaller $\Delta\gamma$ of PSPDTTBT and PCBM will lead to well-mixed films because there is less thermodynamic driving force for phase separation.[32] In order to minimize the Gibbs free energy, the PSPDTTBT and ICBA expel each other developing pronounced phase separation by virtue of the big $\Delta\gamma$.[33]

We noticed there have been a few studies comparing ICBA with PCBM in different polymers. McGehee *et al.* also observed performance reduction using ICBA in a few polymers (PBTTT, PCDTBT, etc.),[34] in which the fullerenes (PCBM and ICBA) have intercalation in polymers. In systems without intercalation like P3HT, or branched PBTTT, there is not performance reduction using ICBA. The intercalation is expected to form trap centers and low mobility, thus reduce efficiency. The PBDTTT-C is not expected to form intercalation with fullerenes, as early GIXRD study on similar polymer (PTB-7) shows no sign of intercalation. McGehee further showed that in PBDT-TPD:fullerene system,[35] replacing PCBM with ICBA leads to insufficient exciton dissociation driving force (small LUMO difference). ICBA photoluminescence (PL) is thus observed, which was explained by energy transfer from polymer to ICBA. In the PBDTTT-C case (bandgap 1.61 eV), the Voc with ICBA is 0.9 V thus the bandgap-Voc offset is 0.71 eV. We have recently showed several polymer (PBDTT-DPP, PBDTT-SeDPP, PDTP-DFBT):PCBM systems[36–38] that bandgap-Voc offset of 0.7 eV can give excellent quantum efficiency (>60%). Thus, the performance reduction in PBDTTT-C:ICBA system is not likely to be due to the insufficient excition dissociation driving force. It will be interesting also to investigate the relationship between polymer CT-state and ICBA triplet state in the future, as when these two states are close, additional loss channel may present.

In summary, we have fabricated the PSPDTTBT:ICBA BHJ solar cells with PCE of 5.21%. Compared with the PSPDTTBT:PCBM device, the higher $J_{SC}$ can be attributed to the morphology improvement induced by the larger surface energy difference ($\Delta\gamma$) between the PSPDTTBT and ICBA. Improved nanoscale morphology results in larger charge mobilities and more balanced carrier transport. These results also point out that synthetic strategies, which adjust the ($\Delta\gamma$) between donor and acceptor, should be considered and has the potential to achieve optimal morphology by tuning the interaction between donor and acceptor molecules.

The authors are grateful to the National Science Council (NSC), Taiwan, (NSC 100-2918-I-001-009) and the Academia Sinica research program on nanoscience and nanotechnology for financial support. The financial support is from Office of Naval Research (Fund number N000141110250), National Science Fundation (DMR-1210893), and UCLA Henry Samuli School of Engineering and Applied Science.

[1]L. M. Chen, Z. Hong, G. Li, and Y. Yang, Adv. Mater. **21**, 1434 (2009).
[2]G. Li, R. Zhu, and Y. Yang, Nature Photon. **6**, 153 (2012).
[3]C. R. McNeill and N. C. Greenham, Adv. Mater. **21**, 3840 (2009).
[4]S. Sista, Z. Hong, L. M. Chen, and Y. Yang, Energy Environ. Sci. **4**, 1606 (2011).
[5]F. He, W. Wang, W. Chen, T. Xu, S. B. Darling, J. Strzalka, Y. Liu, and L. Yu, J. Am. Chem. Soc. **133**, 3284 (2011).
[6]Y. Y. Liang, D. Q. Feng, Y. Wu, S. T. Tsai, G. Li, C. Ray, and L. P. Yu, J. Am. Chem. Soc. **131**, 7792 (2009).
[7]K. H. Ong, S. L. Lim, H. S. Tan, H. K. Wong, J. Li, Z. Ma, L. C. H. Moh, S. H. Lim, J. C. de Mello, and Z. K. Chen, Adv. Mater. **23**, 1409 (2011).
[8]J. Hou, H. Y. Chen, S. Zhang, R. I. Chen, Y. Yang, Y. Wu, and G. Li, J. Am. Chem. Soc. **131**, 15586 (2009).
[9]Y. Y. Liang, Z. Xu, J. Xia, S. T. Tsai, Y. Wu, G. Li, C. Ray, and L. Yu, Adv. Mater. **22**, E135 (2010).
[10]M. K. Siddiki, J. Li, D. Galipeau, and Q. Qiao, Energy Environ. Sci. **3**, 867 (2010).
[11]D. Gendron and M. Leclerc, Energy Environ. Sci. **4**, 1225 (2011).
[12]G. Y. Chen, Y. H. Cheng, Y. J. Chou, M. H. Su, C. M. Chen, and K. H. Wei, Chem. Commun. **47**, 5064 (2011).
[13]J. M. Jiang, P. A. Yang, H. C. Chen, and K. H. Wei, Chem. Commun. **47**, 8877 (2011).
[14]M. C. Scharber, D. Wuhlbacher, M. Koppe, P. Denk, C. Waldauf, A. J. Heeger, and C. L. Brabec, Adv. Mater. **18**, 789 (2006).
[15]Y. He, H. Y. Chen, J. Hou, and Y. Li, J. Am. Chem. Soc. **132**, 1377 (2010).
[16]G. Zhao, Y. He, and Y. Li, Adv. Mater. **22**, 4355 (2010).
[17]D. W. Laird, R. Stegamat, H. Richter, V. Vejins, L. Scott, and T. A. Lada, Patent WO 2008/018931 A2 (2008).
[18]H. Y. Chen, J. Hou, S. Zhang, Y. Liang, G. Yang, Y. Yang, L. Yu, Y. Wu, and G. Li, Nature Photon. **3**, 649 (2009).
[19]J. H. Huang, C. M. Teng, Y. S. Hsiao, F. W. Yen, P. Chen, F. C. Chang, and C. W. Chu, J. Phys. Chem. C **115**, 2398 (2011).
[20]X. Yang, J. Loos, S. C. Veenstra, W. J. H. Verhees, M. M. Wienk, J. M. Kroons, M. A. J. Michels, and R. A. J. Janssen, Nano Lett. **5**, 579 (2005).
[21]J. H. Huang, F. C. Chien, P. Chen, K. C. Ho, and C. W. Chu, Anal. Chem. **82**, 1669 (2010).
[22]J. H. Huang, K. C. Li, F. C. Chien, Y. S. Hsiao, D. Kekuda, P. Chen, H. C. Lin, K. C. Ho, and C. W. Chu, J. Phys. Chem. C **114**, 9062 (2010).
[23]G. Grancini, D. Polli, D. Fazzi, J. C. Gonzalez, G. Cerullo, and G. Lanzani, J. Phys. Chem. Lett. **2**, 1099 (2011).
[24]M. A. Lampart and P. Mark, *Current Injection in Solids* (Academic, New York, 1970).
[25]G. Li, V. Shrotriya, J. Huang, Y. Yao, T. Moriarty, K. Emery, and Y. Yang, Nature Mater. **4**, 864 (2005).
[26]Z. Xu, L. M. Chen, G. Yang, C. H. Huang, J. Hou, Y. Wu, G. Li, C. S. Hsu, and Y. Yang, Adv. Funct. Mater. **19**, 1227 (2009).
[27]J. Y. Oh, W. S. Jang, T. I. Lee, J. M. Myoung, and H. K. Baik, Appl. Phys. Lett. **98**, 023303 (2011).
[28]H. Li, H. Tang, L. Li, W. Xu, X. Zhao, and X. Yang, J. Mater. Chem. **21**, 6563 (2011).
[29]Q. Wei, T. Nishizawa, K. Tajima, and K. Hashimoto, Adv. Mater. **20**, 2211 (2008).
[30]J. W. Jung, J. W. Jo, and W. H. Jo, Adv. Mater. **23**, 1782 (2011).
[31]D. S. Germack, C. K. Chan, B. H. Hamadani, L. J. Richter, D. A. Fischer, D. J. Gundlach, and D. M. DeLongchamp, Appl. Phys. Lett. **94**, 233303 (2009).
[32]J. S. Kim, Y. Lee, J. H. Lee, J. H. Park, J. K. Kim, and K. Cho, Adv. Mater. **22**, 1355 (2010).
[33]C. Z. Li, H. L. Yip, and A. K. Y. Jen, J. Mater. Chem. **22**, 4161 (2012).
[34]N. C. Miller, S. Sweetnam, E. T. Hoke, R. Gysel, C. E. Miller, J. A. Bartelt, X. Xie, M. F. Toney, and M. D. McGehee, Nano Lett. **12**, 1566 (2012).
[35]E. T. Hoke, K. Vandewal, J. A. Bartelt, W. R. Mateker, J. D. Douglas, R. Noriega, K. R. Graham, J. M. J. Fréchet, A. Salleo, and M. D. McGehee, Adv. Energy Mater. **3**, 220 (2013).
[36]L. T. Dou, J. B. You, J. Yang, C.-C. Chen, Y. J. He, S. Murase, T. Moriarty, K. Emery, G. Li, and Y. Yang, Nature Photon. **6**, 180 (2012).
[37]L. Dou, W.-H. Chang, J. Gao, C.-C. Chen, and J. You, Y. Yang, Adv. Mater. **25**, 825 (2013).
[38]J. B. You, L. T. Dou, K. Yoshimura, T. Kato, K. Ohya, T. Moriarty, K. Emery, C.-C. Chen, J. Gao, G. Li, and Y. Yang, Nat. Commun. **4**, 1446 (2013).
[39]See supplementary material at http://dx.doi.org/10.1063/1.4816056 for additional experimental details and results.